Decomposition of 2-Methylfuran. Experimental and Modeling Study

Assa Lifshitz,* Carmen Tamburu, and Ronen Shashua

Department of Physical Chemistry, The Hebrew University, Jerusalem 91904, Israel

Received: August 30, 1996; In Final Form: November 7, 1996[⊗]

The thermal reactions of 2-methylfuran were studied behind reflected shock waves in a pressurized driver single pulse shock tube over the temperature range 1100−1400 K and with overall densities of $\sim 3 \times 10^{-5}$ mol/cm^3. A large number of products resulting from unimolecular cleavage of the ring and consecutive free radical reactions were obtained under shock heating. The unimolecular decomposition is initiated by two parallel channels: (1) 1,2-hydrogen atom migration from C(5) to C(4) and (2) a methyl group migration from C(2) to C(3) in the ring. Each channel is followed by two parallel modes of ring cleavage. In the first channel, breaking the O−C(2) and the C(4)−C(5) bonds in the ring yields CO and different isomers of C_4H_6, whereas breaking of the O−C(2) and the C(3)−C(4) bonds yields CH_2CO and two isomers C_3H_4. In the second channel, breaking the O−C(5), and C(2)−C(3) bonds in the ring yields again CO and isomers of C_4H_6, whereas in the second mode O−C(5), C(2)−C(3), and C(3)−C(4) are broken to yield CO, C_2H_2, and C_2H_4. The four C_4H_6 isomers in decreasing order of abundance were 1,3-butadiene, 1-butyne, 1,2-butadiene, and 2-butyne. The major decomposition product is carbon monoxide. The rate constant for its overall formation is estimated to be $k_{CO} = 10^{15.88} \exp(-78.3 \times 10^3/RT)$ s^{-1}, where R is expressed in units of cal/(K mol). Other products that were found in the postshock samples in decreasing order of abundance were C_4H_4, C_2H_2, CH_4, *p*-C_3H_4, C_2H_6, C_2H_4, *a*-C_3H_4, C_6H_6, C_4H_4O, C_3H_6, and C_4H_2. The total decomposition of 2-methylfuran in terms of a first order rate constant is given by $k_{total} = 10^{14.78} \exp(-71.8 \times 10^3/RT)$ s^{-1}. This rate and the production rate of carbon monoxide are slightly higher than the ones found in the decomposition of furan. An oxygen−carbon mass balance among the decomposition products was obtained. A reaction scheme composed of 36 species and some 100 elementary reactions accounts for the product distribution over the temperature range covered in this study. First order Arrhenius rate parameters for the formation of the various reaction products are given, a reaction scheme is suggested, and results of computer simulation and sensitivity analysis are shown. Differences and similarities in the reactions of furan and 2-methylfuran are discussed.

I. Introduction

We have recently published a detailed investigation of the thermal decomposition of furan in a single pulse shock tube over the temperature range 1060−1260 K and at overall densities of $\sim 3 \times 10^{-5}$ mol/cm^3.[1] It was shown that the main thermal reaction of furan is a 1,2 H atom migration from C(5) to C(4) followed by CO elimination and formation of C_3H_4:

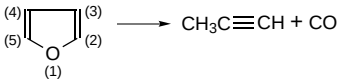

The rate constant obtained for this process was $k_{CO} = 10^{15.25} \exp(-77.5 \times 10^3/RT)$ s^{-1}. Another unimolecular cleavage of the ring produced ketene and acetylene at a rate approximately 3.5 times slower than the production rate of CO and C_3H_4.

In a more recent study we investigated the thermal reactions of 2-furonitrile[2] and found that similar unimolecular ring cleavage takes place where the main products are $CH_3C{\equiv}CCN$ and CO and to a lesser extent $CH{\equiv}CCN$ and CH_2CO. A computer modeling of the overall decomposition of 2-furonitrile, based on a reaction scheme in which these two reactions and a dissociation of the main product, $CH_3C{\equiv}CCN \rightarrow CH_2{\bullet}C{\equiv}CCN + H{\bullet}$, were the major reactions, gave a very good agreement with the experimental results.

We are not aware of any detailed investigations involving other substituted furans such as mono- and dimethylfuran. We are aware, however, of one VLPP study of these molecules[3] where only overall decomposition rates were determined from which high-pressure-limit rate constants were evaluated.

In this investigation we present data on the product distribution in shock heated mixtures of 2-methylfuran with a special emphasis on the C_4H_6 isomers, a detailed mechanism is suggested, a reaction scheme is constructed, and computer simulation including unimolecular decompositions, isomerization, and free radical reactions is performed.

II. Experimental Section

a. Apparatus. The thermal reactions of 2-methylfuran were studied behind reflected shocks in a pressurized driver, 52 mm i.d. single pulse shock tube. The tube and its mode of operation have been described in an earlier publication[4] and will be given here very briefly.

The driven section was 4 m long and was divided in the middle by a 52 mm i.d. ball valve. The driver had a variable length up to a maximum of 2.7 m and could be varied in small steps in order to obtain the most rapid cooling conditions. A 36 L dump tank was connected to the driven section at a 45° angle near the diaphragm holder in order to prevent reflection of transmitted shocks. The driven section was separated from the driver by "Mylar" polyester film of various thickness, depending upon the desired shock strength.

After pumping down the tube to approximately 10^{-5} Torr, the reaction mixture was introduced into the section between the 52 mm i.d. ball valve and the end plate, and pure argon, into the section between the diaphragm and the valve, including the dump tank. Gas samples were collected from the tube through an outlet in the driven section (near the end plate) in

[⊗] Abstract published in *Advance ACS Abstracts,* January 1, 1997.

S1089-5639(96)02646-1 CCC: $14.00

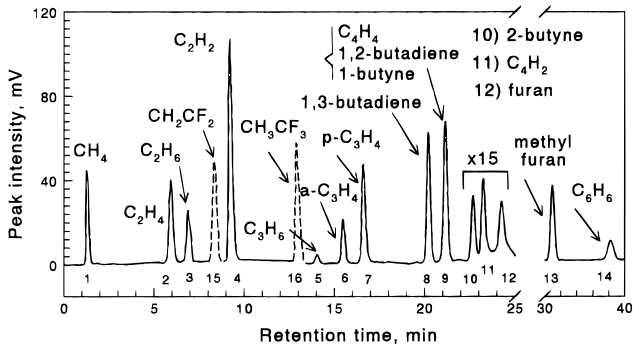

Figure 1. Gas chromatogram of a postshock mixture of 0.5% 2-methylfuran in argon heated to 1319 K.

150 cm^3 glass bulbs and were then analyzed on a Carlo-Erba Model VEGA-2000 gas chromatograph using a flame ionization detector.

Reflected shock temperatures were calculated from the extent of decomposition of 1,1,1-trifluoroethane which was added in small quantities to the reaction mixture and served as an internal standard. Its decomposition to $CH_2{=}CF_2{+}HF$ is a first order unimolecular reaction with a rate constant[5] of $k_{1st} = 10^{14.51}$ exp $(-72.6 \times 10^3/RT)$ s^{-1}.

Reflected shock temperatures were calculated from the relation

$$T = -(E/R)/\left[\ln\left\{-\frac{1}{At}\ln(1-\chi)\right\}\right] \qquad \text{(I)}$$

where t is the reaction dwell time and χ is the extent of decomposition defined as

$$\chi = [CH_2CF_2]_t/([CF_2CH_2]_t + [CH_3CF_3]_t) \qquad \text{(II)}$$

The additional reflected shock parameters were calculated from the measured incident shock velocities using the three conservation equations and the ideal gas equation of state. Dwell times of approximately 1.8 ms were measured with an accuracy of ~5%. Cooling rates were approximately 5×10^5 K/s.

b. Materials and Analysis. Reaction mixtures containing 0.5% 2-methylfuran in argon were prepared manometrically and stored in 12 L glass bulbs at 700 Torr. Both the bulbs and the line were pumped down to $\sim 10^{-5}$ Torr before the preparation of the mixtures. 2-Methylfuran was obtained from Aldrich Chemical Co. and showed only one GC peak. The argon used was Matheson ultrahigh purity grade, listed as 99.9995%, and the helium was Matheson pure grade, listed as 99.999%. All of the materials were used without further purification.

The gas chromatographic analyses of the postshock mixtures were performed on two columns with flame ionization detectors. The analyses of all of the products except for CO were performed on a 2 m Porapak N column. Its initial temperature of 35 °C was gradually elevated to 190 °C in an analysis which lasted about 40 min. A typical chromatogram of 0.5% 2-methylfuran in argon shock heated to 1319 K is shown in Figure 1.

We could not separate the peaks of 1-butyne and 1,2-butadiene from the large peak of C_4H_4. These two C_4H_6 isomers were discovered in an additional series of experiments using GC-MS. In Figure 2 we can see two such chromatograms at 1170 and 1296 K, where *m*/*z* 54, 39, 53, and 27 which are characteristic of the C_4H_6 isomers, and *m*/*z* 52, characteristic of C_4H_4, are shown. As can be seen there are two peaks, slightly separated, of C_4H_6 hidden behind the large peak of C_4H_4. These two peaks were identified as 1,2-butadiene, the first peak, and 1-butyne, the second peak. The identification was based on

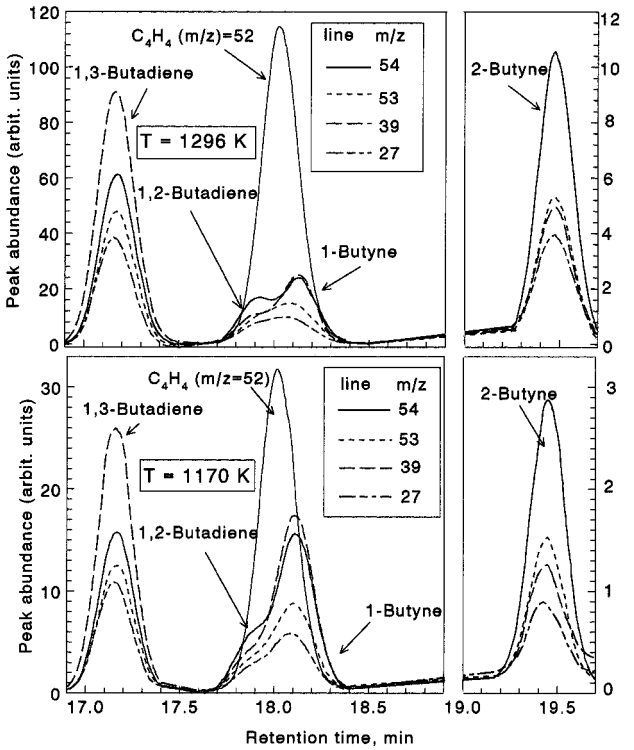

Figure 2. GC/MS chromatograms of the four C_4H_6 isomers at 1170 and 1296 K, respectively. The peaks of 1,2-butadiene and 1-butyne are not separated from the GC peak of C_4H_4.

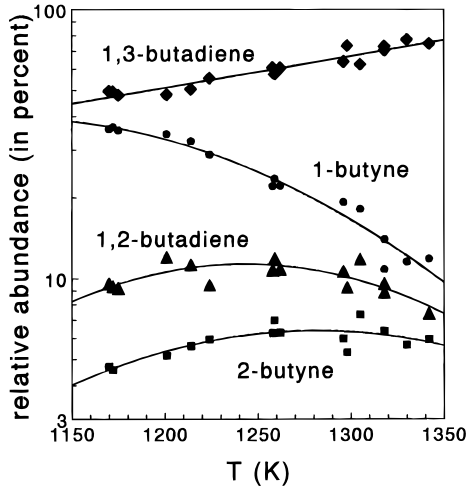

Figure 3. Relative abundance of the four C_4H_6 isomers plotted as a function of temperature.

the relative heights of *m*/*z* 39 and 54 which differ considerably in these two isomers.[6] Figure 3 shows an estimated relative abundance of the four C_4H_6 isomers calculated from the sum of the integrated peak areas of *m*/*z* 54, 39, 53, and 27.

In order to incorporate the GC-MS data into the first series of experiments, we first fitted second order polynomials as a function of T_5 to the GC-MS data points in Figure 3 (shown as lines on the figure) and then used these polynomials to calculate the ratio of the four C_4H_6 isomers in the first series of experiments on the basis of their shock temperature. By using the obtained ratio and knowing the mole percent of 1,3-butadiene, we could calculate the mole percents of 1,2-butadiene and 1-butyne.

We have also carried out another series of experiments in order to verify the presence or absence of ketene and/or methylketene in the postshock mixtures, as these two molecules can be formed in unimolecular decompositions of the ring.

Ketene and methylketene tend to react with small quantities of water absorbed in various locations on the way to the GC and produce acetic and propionic acids, which are also absorbed and hard to analyze. When the postshock mixture is collected in a bulb containing a small quantity of methyl alcohol, methyl acetate is formed from ketene and methyl propionate is formed from methylketene. The latter can be relatively easily, at least qualitatively, analyzed.

We did not identify *any* methyl propionate (methylketene) in the postshock mixtures, but methyl acetate (ketene) was clearly found. The concentration of ketene, which could not be determined quantitatively, was taken as being equal to the sum of allene and propyne, assuming that both molecules are formed with ketene in the same unimolecular process as will be discussed later.

Carbon monoxide was analyzed on a 2 m molecular sieve 5A column at 35 °C. It was reduced at 400 °C to methane prior to its detection using a Chrompak methanyzer with a carrier composed of 50% hydrogen and 50% argon. These analyses gave the ratio [CO]/[CH_4]. From these ratios and the known methane concentration obtained in the Porapak N analyses, the concentration of CO could be calculated for each run. The ratio [CO]/[CH_4] in a standard mixture of methane and carbon monoxide was determined periodically in order to verify a complete conversion of the latter to methane in the methanyzer.

The concentrations of the reaction products $C_5(\mathrm{pr})_i$ were calculated from their GC peak areas from the following relations.[7]

$$C_5(\mathrm{pr}_i) = A(\mathrm{pr}_i)_t/S(\mathrm{pr}_i)\{C_5(\text{2-methylfuran})_0/A(\text{2-methylfuran})_0\} \quad \text{(III)}$$

$$C_5(\text{2-methylfuran})_0 = \{p_1(\%(\text{2-methylfuran}))\rho_5/\rho_1\}/(100RT_1) \quad \text{(IV)}$$

$$A(\text{2-methylfuran})_0 = A(\text{2-methylfuran})_t + {}^1/_5\sum N(\mathrm{pr}_i) \times A(\mathrm{pr}_i)_t/S(\mathrm{pr}_i) \quad \text{(V)}$$

In these relations $C_5(\text{2-methylfuran})_0$ is the concentration of 2-methylfuran behind the reflected shock prior to decomposition and $A(\text{2-methylfuran})_0$ is the calculated GC peak area of 2-methylfuran prior to decomposition (eq V), where $A(\mathrm{pr}_i)_t$ is the peak area of a product i in the shocked sample, $S(\mathrm{pr}_i)$ is its sensitivity relative to 2-methylfuran, and $N(\mathrm{pr}_i)$ is the number of its carbon atoms. ρ_5/ρ_1 is the compression behind the reflected shock, and T_1 is room temperature.

The identification of the reaction products was based on their GC retention times and was also assisted by a Hewlett-Packard Model 5970 mass selective detector. The sensitivities of the various products to the FID were determined relative to 2-methylfuran from standard mixtures. The areas under the GC peaks were integrated with a Spectra Physics Model SP4200 computing integrator and were transferred after each analysis to a PC for data reduction and graphical presentation.

III. Results

In order to determine the distribution of reaction products, some 40 tests were run with mixtures containing 0.5% 2-methylfuran in argon, covering the temperature range 1100−1400 K. Extents of pyrolysis as low as a few hundredths of 1% were determined. Details of the experimental conditions and the distribution of reaction products are given in Table 1. The percent of a given product in the total sample, as shown in the table, corresponds to its mole fraction in the postshock mixture (not including Ar and H_2) and irrespective of the number of its carbon atoms.

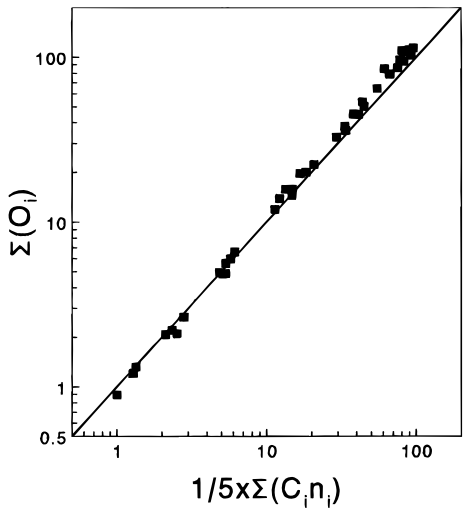

Figure 4. Oxygen−carbon mass balance among the decomposition products.

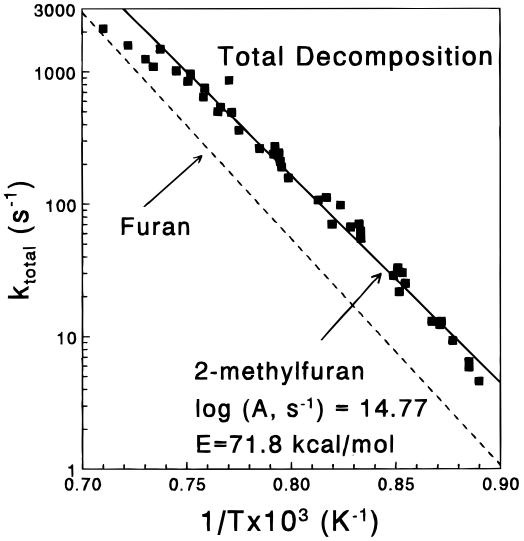

Figure 5. Arrhenius plot of the first order rate constant for the overall decomposition of 2-methylfuran. The rate constant is calculated from the relation $k_{\mathrm{total}} = -\ln\{[\text{2-methylfuran}]_t/[\text{2-methylfuran}]_0\}/t$. The value obtained is $k_{\mathrm{total}} = 10^{14.77} \exp(-71.8 \times 10^3/RT)\ \mathrm{s}^{-1}$. The total decomposition of furan is also shown for comparison.

The balance of oxygen vs carbon among the decomposition products is shown in Figure 4. The concentrations of carbon monoxide, ketene, and furan are plotted against one-fifth of the sum of the concentrations of all of the decomposition products (including the oxygen containing species), each multiplied by the number of its carbon atoms. One-fifth is the ratio of oxygen to carbon in the reactant molecule. The 45° line in the figure represents a complete mass balance. As can be seen there is no major deviation from an oxygen−carbon balance over the temperature range of the investigation.

Figure 5 shows the rate constant for the overall decompositions of 2-methylfuran, calculated as a first order rate constant from the relation:

$$k_{\mathrm{total}} = -\ln\{[\text{2-methylfuran}]_t / [\text{2-methylfuran}]_0\}/t \quad \text{(VI)}$$

The value obtained is $k_{\mathrm{total}} = 10^{14.78} \exp(-71.8 \times 10^3/RT)\ \mathrm{s}^{-1}$, where R is expressed in units of cal/(K mol). The rate constant for the total decomposition of furan is also shown on the graph

TABLE 1: Experimental Conditions and Product Distribution in Percent

shock no.	T_5, K	dwell time, ms	$C_5 \times 10^5$	product distribution																
				2-methylfuran	CO	CH_4	C_2H_4	1,3-butadiene	1,2-butadiene	1-butyne	2-butyne	C_4H_4	C_4H_2	furan	C_2H_6	C_2H_2	C_3H_6	allene	propyne	CH_2CO	C_6H_6
1	1124	2.20	3.14	97.95	0.652	0.171	0.0590	0.204	0.0327	0.223	0.0082	0.167		0.159	0.0445	0.184		0.0082	0.0659	0.0742	
2	1130	2.20	3.10	97.31	0.922	0.214	0.0702	0.249	0.0485	0.265	0.0096	0.253		0.151	0.0491	0.235		0.0224	0.0924	0.115	
3	1130	2.10	2.72	97.33	0.827	0.221	0.0885	0.214	0.0424	0.228	0.0655	0.175		0.389	0.0468	0.207		0.0139	0.0695	0.0834	
4	1140	2.30	2.75	95.46	1.63	0.355	0.125	0.404	0.0707	0.409	0.0243	0.410		0.190	0.109	0.404		0.0288	0.173	0.202	
5	1147	1.82	2.77	94.85	1.85	0.439	0.166	0.497	0.0898	0.485		0.433			0.103	0.479	0.0332	0.0454	0.241	0.287	
6	1148	2.10	2.77	95.37	0.970	0.397	0.136	0.468	0.0850	0.456	0.0212	0.205		0.865	0.135	0.389	0.0504	0.0505	0.169	0.220	
7	1153	2.20	3.04	94.03	2.08	0.477	0.164	0.535	0.0991	0.506	0.0262	0.603		0.199	0.137	0.568		0.0404	0.241	0.282	
8	1170	2.09	2.82	89.19	3.87	0.818	0.312	0.960	0.188	0.812	0.0652	1.01			0.254	1.02	0.0439	0.127	0.567	0.692	0.0774
9	1172	1.81	2.78	88.43	4.49	0.914	0.327	0.951	0.187	0.798	0.0616	0.985		0.0779	0.252	1.04	0.0437	0.126	0.567	0.691	0.0737
10	1174	2.30	2.88	89.69	3.83	0.719	0.257	0.836	0.166	0.693	0.0639	1.12		0.232	0.296	0.88		0.0995	0.489	0.590	0.0184
11	1175	1.79	2.95	87.69	4.75	0.956	0.346	1.01	0.201	0.833	0.0645	1.07		0.0664	0.249	1.09	0.0484	0.141	0.605	0.745	0.125
12	1178	2.20	2.76	86.86	5.04	0.936	0.338	0.889	0.178	0.719	0.0692	1.56		0.254	0.360	1.15		0.149	0.659	0.807	
13	1200	2.20	2.72	75.00	11.35	1.56	0.704	1.54	0.316	1.05	0.115	1.68		0.748	0.775	2.02	0.171	0.330	1.13	1.46	
14	1200	2.20	2.43	77.26	8.52	1.55	0.554	1.75	0.361	1.21	0.134	2.37	0.0126	0.313	0.587	2.03		0.315	1.27	1.58	0.136
15	1201	1.83	2.64	75.20	9.95	1.81	0.670	1.81	0.372	1.23	0.131	2.18		0.268	0.590	2.18	0.0949	0.342	1.34	1.68	0.150
16	1207	2.30	2.35	73.82	10.08	1.90	0.705	1.82	0.376	1.18	0.199	2.47	0.0248	0.539	0.689	2.35	0.0936	0.417	1.42	1.83	
17	1214	1.87	2.63	67.39	13.24	2.34	0.916	2.32	0.477	1.43	0.177	2.65	0.0196	0.380	0.797	2.84	0.122	0.521	1.82	2.34	0.238
18	1220	2.30	2.69	71.33	10.70	1.78	0.694	2.15	0.441	1.26	0.193	2.96	0.0193	0.314	0.838	2.61		0.517	1.72	2.23	0.186
19	1224	1.80	2.65	65.70	13.40	2.31	0.937	2.35	0.477	1.33	0.176	3.82	0.0256	0.235	0.907	2.90	0.122	0.589	1.89	2.48	0.350
20	1230	2.10	2.39	63.24	14.53	2.56	1.01	2.52	0.508	1.34	0.234	3.31	0.0249	0.573	0.110	3.37	0.151	0.676	2.08	2.75	0.930
21	1252	2.20	2.50	50.47	18.88	3.17	1.34	3.59	0.685	1.44	0.306	4.55	0.0520	0.364	1.55	4.80		1.04	3.09	4.14	0.367
22	1257	2.10	2.30	46.60	20.50	3.69	1.65	3.60	0.673	1.49	0.329	4.09	0.0805	0.601	1.63	4.93	0.199	1.12	3.07	4.17	1.38
23	1258	1.94	2.56	45.71	21.56	3.58	1.68	3.71	0.693	1.52	0.317	3.87	0.0986	0.334	1.63	5.11	0.215	1.12	3.16	4.28	1.41
24	1259	1.96	2.20	40.17	24.23	4.14	1.89	3.99	0.566	0.846	0.323	5.22	0.103	0.398	1.77	5.58	0.238	1.25	3.46	4.71	1.10
25	1262	2.10	2.34	34.49	27.10	4.51	2.17	4.21	0.774	1.65	0.326	4.38	0.123	0.474	1.90	6.22	0.267	1.37	3.73	5.10	1.22
26	1263	2.15	2.20	38.52	24.03	4.35	1.98	4.05	0.742	1.57	0.356	4.89	0.0928	0.551	1.96	5.89	0.226	1.32	3.52	4.81	1.34
27	1274	2.20	2.33	34.65	25.60	4.40	2.16	4.39	0.758	1.50	0.384	4.57	0.104	0.551	2.27	6.39	0.292	1.48	3.82	5.29	1.42
28	1290	2.20	2.49	25.14	29.29	5.10	2.71	5.23	0.830	1.50	0.340	5.02	0.192	0.358	2.63	8.11		1.75	4.49	6.25	0.993
29	1296	1.92	2.32	19.22	36.23	6.15	3.07	4.57	0.697	1.22	0.241	4.35	0.157	0.487	2.58	8.53	0.317	1.52	4.09	5.62	0.951
30	1298	1.88	2.30	8.44	40.89	6.93	4.27	4.23	0.637	1.11	0.214	4.09	0.404	0.324	2.66	11.40	0.383	1.75	4.17	5.92	2.18
31	1305	2.00	2.47	17.15	33.78	5.79	3.83	4.61	0.662	1.11	0.296	5.33	0.334	0.382	2.61	9.24	0.233	1.74	4.36	6.10	2.44
32	1307	2.20	2.36	16.70	32.55	5.81	3.52	5.55	0.785	1.30	0.307	5.09	0.314	0.315	2.95	9.83		1.94	4.82	6.77	1.38
33	1318	2.00	2.30	10.11	37.45	6.57	4.42	5.19	0.674	1.06	0.231	5.09	0.404	0.302	2.77	10.60	0.249	1.80	4.41	6.21	2.45
34	1319	2.10	1.99	12.06	35.25	6.92	4.41	4.93	0.633	0.994	0.247	4.56	0.308	0.337	2.85	10.79	0.342	1.86	4.42	6.25	2.48
35	1330	1.81	2.11	7.44	40.07	7.26	4.61	4.16	0.487	0.727	0.199	4.54	0.480	0.298	2.63	12.27	0.371	1.76	4.10	5.87	2.71
36	1332	2.00	2.16	8.14	36.73	6.78	4.76	5.30	0.606	0.900	0.259	4.80	0.418	0.247	3.21	11.65	0.318	1.97	4.62	6.57	2.39
37	1342	2.00	2.23	5.50	39.63	7.45	5.52	4.01	0.416	0.594	0.166	4.98	0.654	0.189	2.54	13.25	0.362	1.68	3.97	5.65	3.43
38	1356	2.00	1.86	1.93	40.08	8.44	6.40	3.59	0.322	0.438	0.123	3.98	0.539	0.0938	2.69	15.47	0.319	1.66	3.83	8.53	1.40
39	1362	2.00	1.76	4.48	38.15	8.30	6.33	2.76	0.235	0.307	0.102	3.78	0.780	0.128	2.04	16.51	0.261	1.44	3.18	8.05	2.85
40	1369	2.05	1.86	3.17	36.52	7.89	6.68	3.05	0.236	0.306	0.135	4.43	0.909	0.0842	2.22	17.42	0.265	1.53	3.43	7.69	3.75
41	1385	1.95	1.60	1.71	37.10	8.56	7.12	1.64	0.103	0.127	0.0721	3.08	1.33	0.0381	1.28	23.08	0.194	1.13	2.47	7.82	2.96
42	1408	1.75	1.43	0.851	37.59	8.66	6.68	0.658	0.0300	0.0354	0.0263	1.53	1.77	0.0119	0.554	29.20	0.110	0.722	1.56	8.06	1.61

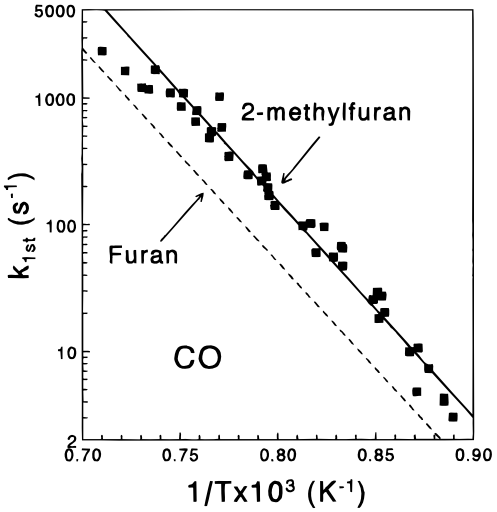

Figure 6. Arrhenius plot of the first order production of carbon monoxide. The rate constant is calculated from the relation $k_{product} = k_{total} \times [product]_t/([2\text{-methylfuran}]_0 - [2\text{-methylfuran}]_t)$. The production rate of carbon monoxide in furan is also shown for comparison.

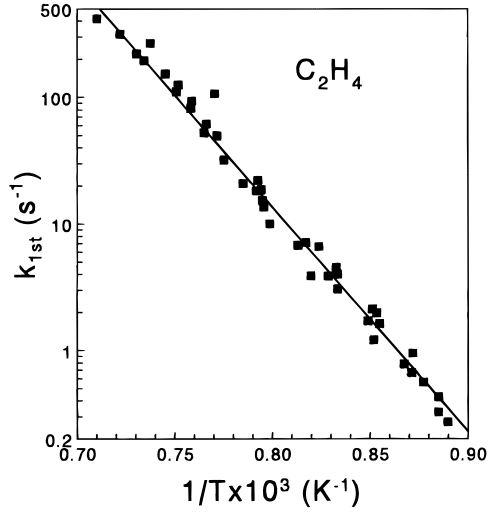

Figure 7. Arrhenius plots of the rate of the production of ethylene.

for comparison. The overall decomposition of 2-methylfuran is somewhat faster owing to faster initiation of free radical reactions due to the existence of a methyl group in the molecule. Figures 6−8 show Arrhenius plots of the first order production rate of CO and of two other decomposition products, calculated from the relation

$$k_{product} = \frac{[product]_t}{[2\text{-methylfuran}]_0 - [2\text{-methylfuran}]_t} k_{total} \quad \text{(VII)}$$

Figure 6 shows also the production rate of CO in furan for comparison. The rate in 2-methylfuran is slightly higher owing to an additional channel in its production. This will be discussed later.

Values of E obtained from the slopes of the lines and their corresponding preexponential factors are summarized in Table 2. It should be mentioned that the parameters for the decomposition products do not represent elementary unimolecular reactions. Moreover, even for true unimolecular decompositions such as the formation of the various C_4H_6 isomers the rates are not the true unimolecular formation rates because of the further decomposition of these compounds at higher temperatures. This presentation simply provides a way of summarizing general rates. Also, it does not imply that the overall decomposition

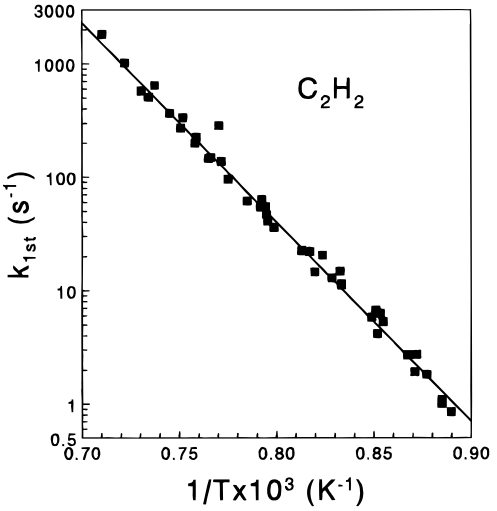

Figure 8. Arrhenius plot of the rate of the production acetylene.

TABLE 2: Arrhenius Parameters for Production Rates

compound	log{A, s^{-1}}	E, kcal/mol
total decomposn	14.78	71.8
CO	15.88	78.3
CH_4	13.95	71.6
C_2H_4	15.50	82.2
C_2H_6	15.49	82.5
C_2H_2	15.70	80.6
C_3H_6	10.69	59.9
$CH_2{=}C{=}CH_2$	17.10	93.1
$CH_3C{\equiv}CH$	15.39	80.5
$CH_2{=}CHCH{=}CH_2$	13.74	70.3
$CH_2{=}C{=}CHCH_3$	15.11	81.6
$CH{\equiv}CCH_2CH_3$	12.10	62.0
$CH_3C{\equiv}CCH_3$	15.46	86.3
C_4H_4	16.38	84.6
C_4H_2	20.72	120
C_4H_4O	6.41	33.7
C_6H_6	17.56	96.4
$CH_2{=}CO$	15.91	82.8

of 2-methylfuran under the conditions of the present experiment is a simple unimolecular process. As will be discussed later, the decomposition is composed of a large number of elementary steps involving unimolecular and free radical reactions.

IV. Discussion

a. Unimolecular Processes. It has recently been shown[1] that the major unimolecular channel in the decomposition of furan is a 1,2 H-atom migration from C(5) to C(4) in the ring, followed by elimination of carbon monoxide and formation of C_3H_4 (Scheme 1). The large preexponential factor and activation energy of this reaction, as obtained from the production rate of CO[1], $k_{(furan \rightarrow C_3H_4+CO)} = 10^{15.25} \exp(-77.5 \times 10^3/RT)\ s^{-1}$, clearly point to the existence of a biradical mechanism where the O(1)—C(2) bond in the ring must be almost completely broken prior to the rearrangements in the open ring structure and elimination of CO.

The formation of a stable C_3H_4 molecule which follows the ring opening requires an H-atom migration from C(3) to either C(4) or C(2). A migration to C(4) leads to the formation of methylacetylene, and a migration to C(2), to the formation allene. Both structural isomers were found in mixtures of shock heated furan.

The ratio [methylacetylene]/[allene] was around 10 at low temperatures. Owing to allene → methylacetylene isomerization ($k_{isomerization} = 10^{13.17} \exp[-60.4 \times 10^3/RT]\ s^{-1}$)[8], it approached a value of ∼3 at high temperatures, which is roughly the equilibrium ratio.[9] It is thus obvious that the preferred H-atom

SCHEME 1

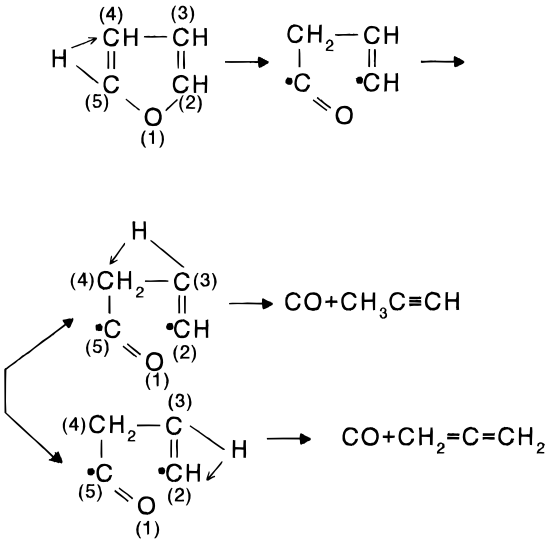

SCHEME 2

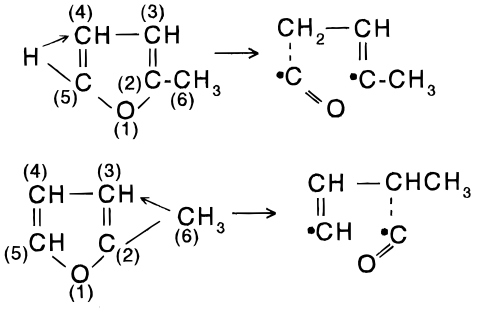

migration is a migration from C(3) to C(4), even beyond the thermal stability of these two isomers.

The results obtained in the study of 2-methylfuran show that CO elimination from the ring in 2-methylfuran follows a pattern similar to that of furan. However, the loss of symmetry in 2-methylfuran opens additional channels. The process thus starts in 2-methylfuran by a 1,2 H-atom migration from C(5) to C(4) but can also take place by a 1,2 methyl group migration from C(2) to C(3) (Scheme 2). The question of whether the latter does indeed exist will be dealt with after the results of the computer simulation are described.

In addition to CO, both channels lead also to the production of C_4H_6 intermediates. In order to obtain stable C_4H_6 molecules, additional rearrangements must take place in the remaining open ring structures. These structures are CO···C(4)H_2•—C(3)H═C(2)•—C(6)H_3, in the first channel (H-atom migration), and C(5)H•═C(4)H—C(3)(···CO)H•—C(6)H_3, in the second channel (methyl group migration).

There are three possibilities for rearranging and stabilizing the first intermediate, CO···C(4)H_2•—C(3)H═C(2)•—C(6)H_3, by additional 1,2 H-atom migrations (Scheme 3).

Migration from

(1) C(6) to C(2) yields CO + CH_2═CHCH═CH_2 1,3-butadiene

(2) C(3) to C(4) yields CO + CH_3C≡CCH_3 2-butyne

(3) C(3) to C(2) yields CO + CH_2═C═$CHCH_3$ 1,2-butadiene

We cannot visualize a production of 1-butyne, CH≡CCH_2CH_3,

SCHEME 3

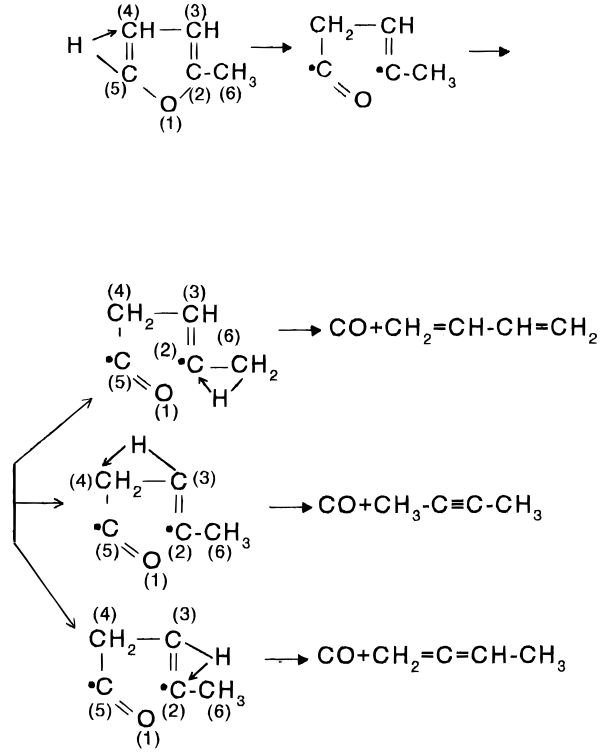

SCHEME 4

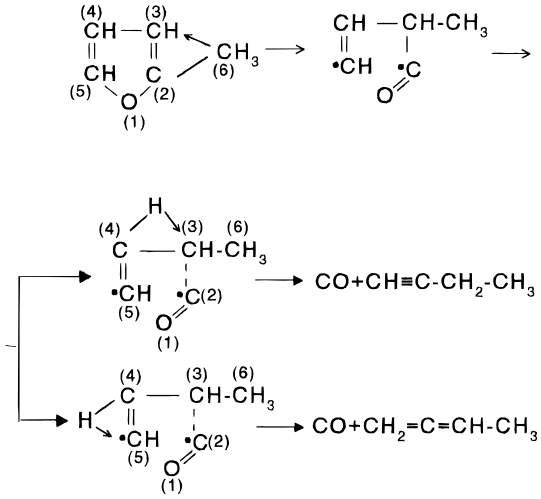

from this intermediate by a simple rearrangement. We have thus assumed that it is not formed in the 1,2 H-atom migration channel.

There are two possibilities for stabilizing the second intermediate, C(5)H•═C(4)H—C(3)(···CO)H•—C(6)H_3, by additional 1,2 H-atom migrations (Scheme 4).

Migration from

(1) C(4) to C(3) yields CO + CH≡CCH_2CH_3 1-butyne

(2) C(4) to C(5) yields CO + CH_2═C═$CHCH_3$ 1,2-butadiene

Similarly, we cannot see how 1,3-butadiene, CH_2═CHCH═CH_2, and 2-butyne, CH_3C≡CCH_3, can be formed from this intermediate by simple rearrangements.

TABLE 3: Reaction Scheme for the Decomposition of 2-Methylfuran[a]

reaction	A	n	E	k_f(1250 K)	k_r(1250 K)	$\Delta S_r°$(1250 K)	$\Delta H_r°$(1250 K)	ref
1. 2-mf → $CH_3C{\equiv}CCH_3 + CO$	2.25×10^{15}	0	85.1	2.98	4.16	42.0	24.7	this work
2. 2-mf → $CH_2{=}CHCH{=}CH_2 + CO$	3.50×10^{15}	0	79.5	4.42×10	9.68×10^{-1}	43.9	16.8	this work
3. 2-mf → $CH_2{=}C{=}CH{-}CH_3 + CO$	4.50×10^{15}	0	85.1	5.96	1.02×10	45.5	29.6	this work
4. 2-mf → $CH{\equiv}C{-}CH_2CH_3 + CO$	2.80×10^{15}	0	79.5	3.53×10	9.88×10	45.2	30.3	this work
5. 2-mf → *p*-$C_3H_4 + CH_2CO$	5.75×10^{15}	0	82.9	1.85×10	6.62×10^{4}	46.3	49.5	this work
6. 2-mf → $C_2H_2 + C_2H_4 + CO$	1.70×10^{15}	0	79.5	2.15×10	4.03×10^{4}	76.7	57.2	this work
7. 2-mf → $CH_3CO + C_3H_3$	4.00×10^{16}	0	90.5	6.03	6.10×10^{10}	52.7	94.5	estd
8. 2-mf → $HCO + CH{=}CHCH{=}CH_2$	4.00×10^{16}	0	106.0	1.18×10^{-2}	1.35×10^{11}	51.8	110.7	estd
9. 2-mf → 2-mfuryl + H	1.60×10^{16}	0	86.0	1.48×10	6.74×10^{14}	32.8	90.5	estd
10. 2-mf + H → 2-mfuryl + H_2	3.00×10^{14}	0	9.00	8.01×10^{12}	8.08×10^{8}	5.19	−16.4	estd
11. 2-mf + CH_3 → 2-mfuryl + CH_4	1.50×10^{12}	0	10.0	2.68×10^{10}	5.18×10^{7}	−1.39	−17.3	estd
12. 2-mf + C_3H_3 → 2-mfuryl + *p*-C_3H_4	8.00×10^{11}	0	10.0	1.43×10^{10}	5.43×10^{9}	−0.144	−2.58	estd
13. 2-mf + C_3H_3 → 2-mfuryl + *a*-C_3H_4	8.00×10^{11}	0	10.0	1.43×10^{10}	1.65×10^{10}	−1.18	−1.12	estd
14. 2-mf + C_3H_5 → 2-mfuryl + C_3H_6	8.00×10^{11}	0	12.0	6.38×10^{9}	1.19×10^{10}	−1.15	0.116	estd
15. 2-mf + C_4H_3 → C_4H_4 + 2-mfuryl	8.00×10^{11}	0	8.00	3.19×10^{10}	3.80×10^{7}	−0.158	−16.9	estd
16. 2-mf + H → furan + CH_3	5.00×10^{14}	0	8.00	2.00×10^{13}	1.07×10^{11}	2.52	−9.84	estd
17. furan → *p*-C_3H_4 + CO	1.78×10^{15}	0	75.0	1.38×10^{2}	1.20×10	48.2	25.5	1
18. furan → $C_2H_2 + CH_2CO$	5.01×10^{14}	0	77.5	1.41×10	1.83×10^{4}	49.3	50.8	1
19. furan → C_3H_3 + HCO	4.00×10^{16}	0	100.5	1.08×10^{-1}	2.91×10^{9}	56.0	101	estd
20. 2-mfuryl → $CO + CH_2{=}C{=}CHCH_2$	4.00×10^{15}	0	64.0	2.59×10^{4}	6.95×10^{4}	45.0	30.	estd
21. 2-mfuryl → $CO + CH{=}CHCH{=}CH_2$	2.25×10^{15}	0	71.0	8.70×10^{2}	8.48×10^{4}	44.1	37.9	estd
22. 2-mfuryl → $CH_2CO + C_3H_3$	2.25×10^{15}	0	64.0	1.46×10^{4}	1.37×10^{8}	46.4	52.1	estd
23. 2-mfuryl → $HCO + C_4H_4$	2.25×10^{15}	0	64.0	1.46×10^{4}	1.52×10^{10}	47.4	65.1	estd
24. 2-mfuryl → $C_2H_2 + C_2H_3 + CO$	3.29×10^{15}	0	76.7	1.28×10^{2}	9.34×10^{8}	79.1	80.9	estd
25. $CH_3C{\equiv}CCH_3$ → $CH_2{=}CHCH{=}CH_2$	3.00×10^{13}	0	65.0	1.30×10^{2}	2.04	1.95	−7.89	17
26. $CH_2{=}C{=}CHCH_3$ → $CH_2{=}CHCH{=}CH_2$	3.00×10^{13}	0	65.0	1.30×10^{2}	1.66	−1.56	−12.8	17
27. $CH_2{=}C{=}CHCH_3$ → $CH_3C{\equiv}CCH_3$	3.00×10^{13}	0	65.0	1.30×10^{2}	1.06×10^{2}	−3.51	−4.9	17
28. $CH{\equiv}C{-}CH_2CH_3$ → $CH_2{=}C{=}CHCH_3$	3.00×10^{13}	0	65.0	1.30×10^{2}	7.96×10	0.357	−0.769	17
29. $CH_3C{\equiv}CCH_3$ → $CH_2{-}C{\equiv}CCH_3 + H$	6.00×10^{15}	0	94.0	2.21×10^{-1}	3.20×10^{12}	38.1	94.2	estd
30. $CH_2{=}CHCH{=}CH_2$ → $CH{=}CHCH{=}CH_2 + H$	4.00×10^{15}	0	111.0	1.57×10^{-4}	3.19×10^{13}	33.0	111.6	estd
31. $CH_2{=}CHCH{=}CH_2$ → $CH_2{=}C{=}CHCH_2 + H$	2.00×10^{15}	0	103.0	1.97×10^{-3}	1.10×10^{13}	33.8	103.7	estd
32. $CH_2{=}C{=}CHCH_3$ → $CH_2C{\equiv}C{-}CH_3 + H$	1.00×10^{15}	0	89.0	2.76×10^{-1}	3.25×10^{12}	34.6	89.3	estd
33. $CH_2{=}C{=}CHCH_3$ → $CH_2{=}C{=}CHCH_2 + H$	3.00×10^{15}	0	91.0	3.70×10^{-1}	2.64×10^{13}	32.3	90.9	estd
34. $CH{\equiv}CCH_2CH_3$ → $CH{\equiv}CCHCH_3 + H$	2.00×10^{15}	0	72.0	5.17×10^{2}	5.37×10^{15}	34.9	89.5	estd
35. $CH{\equiv}CCH_2CH_3$ → $CH{\equiv}CCH_2CH_2 + H$	3.00×10^{15}	0	101.0	6.60×10^{-3}	5.41×10^{12}	35.5	101.1	estd
36. $CH_2{=}C{=}CHCH_3$ → $C_3H_3 + CH_3$	1.00×10^{16}	0	79.0	1.54×10^{2}	5.04×10^{12}	38.2	79.2	estd
37. $CH{\equiv}CCH_2CH_3$ → $C_3H_3 + CH_3$	1.00×10^{16}	0	78.0	2.31×10^{2}	4.62×10^{12}	38.5	78.4	estd
38. $CH_3C{\equiv}CCH_3 + H$ → $CH_2C{\equiv}CCH_3 + H_2$	6.00×10^{14}	0	6.80	3.88×10^{13}	1.24×10^{9}	10.4	−12.7	estd
39. $CH_2{=}CHCH{=}CH_2 + H$ → $CH{=}CHCH{=}CH_2 + H_2$	4.00×10^{14}	0	6.80	2.59×10^{13}	1.16×10^{13}	5.38	4.74	estd
40. $CH_2{=}CHCH{=}CH_2 + H$ → $CH_2{=}C{=}CHCH_2 + H_2$	2.00×10^{14}	0	6.80	1.29×10^{13}	1.60×10^{11}	6.20	−3.16	estd
41. $CH_2{=}C{=}CHCH_3 + H$ → $CH_2C{\equiv}CCH_3 + H_2$	1.00×10^{14}	0	6.80	6.47×10^{12}	1.69×10^{8}	6.94	−17.5	estd
42. $CH_2{=}C{=}CHCH_3 + H$ → $CH_2{=}C{=}CHCH_2 + H_2$	3.00×10^{14}	0	6.80	1.94×10^{13}	3.07×10^{9}	4.64	−15.9	estd
43. $CH{\equiv}CCH_2CH_3 + H$ → $CH{\equiv}CCHCH_3 + H_2$	2.00×10^{14}	0	6.80	1.29×10^{13}	2.97×10^{8}	7.29	−17.4	estd
44. $CH{\equiv}CCH_2CH_3 + H$ → $CH{\equiv}CCH_2CH_2 + H_2$	3.00×10^{14}	0	6.80	1.94×10^{13}	3.52×10^{10}	7.89	−5.82	estd
45. $CH_3C{\equiv}CCH_3 + CH_3$ → $CH_4 + CH_2C{\equiv}CCH_3$	6.00×10^{13}	0	11.5	5.86×10^{11}	3.59×10^{8}	3.87	−13.5	estd
46. $CH_2{=}CHCH{=}CH_2 + CH_3$ → $CH_4 + CH_2{=}C{=}CHCH_2$	4.00×10^{13}	0	11.5	3.90×10^{11}	9.25×10^{10}	−0.377	−4.05	estd
47. $CH_2{=}CHCH{=}CH_2 + CH_3$ → $CH_4 + CH{=}CHCH{=}CH_2$	2.00×10^{13}	0	11.5	1.95×10^{11}	1.68×10^{12}	−1.20	3.85	estd
48. $CH_2{=}C{=}CHCH_3 + CH_3$ → $CH_4 + CH_2C{\equiv}CCH_3$	1.00×10^{13}	0	11.5	9.76×10^{10}	4.88×10^{7}	0.358	−18.4	estd
49. $CH_2{=}C{=}CHCH_3 + CH_3$ → $CH_4 + CH_2{=}C{=}CHCH_2$	3.00×10^{13}	0	11.5	2.93×10^{11}	8.86×10^{8}	−1.94	−16.8	estd
50. $CH{\equiv}CCH_2CH_3 + CH_3$ → $CH_4 + CH{\equiv}CCHCH_3$	2.00×10^{13}	0	11.5	1.95×10^{11}	8.59×10^{7}	0.716	−18.3	estd
51. $CH{\equiv}CCH_2CH_3 + CH_3$ → $CH_4 + CH{\equiv}CCH_2CH_2$	3.00×10^{13}	0	11.5	2.93×10^{11}	1.02×10^{10}	1.32	−6.7	estd
52. $CH_3C{\equiv}CCH_3 + C_3H_3$ → *p*-$C_3H_4 + CH_2C{\equiv}CCH_3$	3.00×10^{13}	0	11.5	2.93×10^{11}	3.53×10^{10}	5.12	1.14	estd
53. $CH_2{=}CHCH{=}CH_2 + C_3H_3$ → *p*-$C_3H_4 + CH_2{=}C{=}CHCH_2$	2.00×10^{13}	0	19.0	9.53×10^{9}	4.44×10^{11}	0.872	10.6	estd
54. $CH_2{=}CHCH{=}CH_2 + C_3H_3$ → *p*-$C_3H_4 + CH{=}CHCH{=}CH_2$	1.00×10^{13}	0	12.0	7.98×10^{10}	1.35×10^{14}	0.052	18.5	estd

TABLE 3 (Continued)

reaction	A	n	E	k_f(1250 K)	k_r(1250 K)	$\Delta S_r°$(1250 K)	$\Delta H_r°$(1250 K)	ref
55. $CH_2{=}C{=}CHCH_3 + C_3H_3 \rightarrow p\text{-}C_3H_4 + CH_2C{\equiv}CCH_3$	5.00×10^{12}	0	12.0	3.99×10^{10}	3.92×10^{9}	1.61	−3.76	estd
56. $CH_2{=}C{=}CHCH_3 + C_3H_3 \rightarrow p\text{-}C_3H_4 + CH_2{=}C{=}CHCH_2$	1.50×10^{13}	0	12.0	1.20×10^{11}	7.12×10^{10}	−0.693	−2.16	estd
57. $CH{\equiv}CCH_2CH_3 + C_3H_3 \rightarrow p\text{-}C_3H_4 + CH{\equiv}CCHCH_3$	1.00×10^{13}	0	12.0	7.98×10^{10}	6.90×10^{9}	1.97	−3.62	estd
58. $CH{\equiv}CCH_2CH_3 + C_3H_3 \rightarrow p\text{-}C_3H_4 + CH{\equiv}CCH_2CH_2$	1.50×10^{13}	0	12.0	1.20×10^{11}	8.17×10^{11}	2.57	7.98	estd
59. $CH_2{=}CHCH{=}CH_2 \rightarrow C_4H_4 + H_2$	2.00×10^{13}	0	75.0	1.55	2.88×10^{6}	33.88	49.6	17
60. $a\text{-}C_3H_4 \rightarrow p\text{-}C_3H_4$	1.48×10^{13}	0	60.4	4.08×10^{2}	1.34×10^{2}	1.03	−1.47	8
61. $a\text{-}C_3H_4 + Ar \rightarrow C_3H_3 + H + Ar$	4.05×10^{17}	0	75.0	3.13×10^{4}	1.24×10^{18}	34.0	91.6	12
62. $p\text{-}C_3H_4 + Ar \rightarrow C_3H_3 + H + Ar$	4.70×10^{17}	0	80.0	4.85×10^{3}	5.83×10^{17}	33.0	93.1	19
63. $p\text{-}C_3H_4 + H \rightarrow C_3H_5$	2.00×10^{13}	0	2.40	7.61×10^{12}	1.36×10^{3}	−24.7	−57.9	20
64. $a\text{-}C_3H_4 + H \rightarrow C_3H_5$	2.00×10^{13}	0	2.40	7.61×10^{12}	4.49×10^{2}	−23.7	−59.4	20
65. $p\text{-}C_3H_4 + C_3H_3 \rightarrow C_6H_6 + H$	7.00×10^{12}	0	10.0	1.25×10^{11}	4.35×10^{7}	−27.2	−53.7	estd
66. $CH{\equiv}CCHCH_3 \rightarrow H + C_4H_4$	1.00×10^{14}	0	74.0	1.16×10	7.35×10^{9}	25.4	53.4	estd
67. $CH_2C{\equiv}CCH_3 \rightarrow H + C_4H_4$	1.00×10^{14}	0	54.0	3.62×10^{4}	3.31×10^{13}	25.4	54.3	estd
68. $CH{\equiv}CCH_2CH_2 \rightarrow H + C_4H_4$	1.00×10^{14}	0	42.0	4.54×10^{6}	3.66×10^{13}	24.8	41.8	estd
69. $CH{=}CHCH{=}CH_2 \rightarrow H + C_4H_4$	1.00×10^{14}	0	45.0	1.36×10^{6}	5.64×10^{12}	28.5	44.8	estd
70. $CH_2{=}C{=}CHCH_2 \rightarrow H + C_4H_4$	1.00×10^{14}	0	53.0	5.42×10^{4}	8.18×10^{12}	27.7	52.7	estd
71. $CH_2{=}CHCH{=}CH_2 \rightarrow C_2H_2 + C_2H_4$	1.20×10^{13}	0	66.0	3.47×10	2.98×10^{6}	32.7	40.4	17
72. $C_2H_2 + C_2H_2 \rightarrow C_4H_4$	6.20×10^{13}	0	41.1	4.05×10^{6}	1.01×10^{2}	−30.3	−35.5	12
73. $C_2H_2 + C_2H_2 \rightarrow C_4H_3 + H$	1.00×10^{12}	0	66.0	2.89	2.78×10^{12}	2.68	71.9	21
74. $CH_3 + C_2H_2 \rightarrow C_3H_5$	6.03×10^{11}	0	7.70	2.71×10^{10}	2.51×10^{3}	−30.3	−49.4	13
75. $C_2H_3 + Ar \rightarrow C_2H_2 + H + Ar$	2.50×10^{15}	0	33.6	3.34×10^{9}	7.41×10^{15}	23.8	37.4	12
76. $C_2H_3 + H \rightarrow C_2H_2 + H_2$	8.00×10^{13}	0	0	8.00×10^{13}	3.92×10^{2}	−3.83	−69.5	13
77. $C_2H_3 + CH_3 \rightarrow C_2H_2 + CH_4$	3.92×10^{11}	0	0	3.92×10^{11}	3.68×10	−10.4	−70.4	13
78. $C_2H_3 + CH_3 \rightarrow C_3H_6$	7.23×10^{13}	0	0	7.23×10^{13}	6.07×10^{-1}	−40.4	−102.4	22
79. $HCO + Ar \rightarrow H + CO + Ar$	2.50×10^{14}	0	16.9	2.78×10^{11}	1.07×10^{14}	25.2	17.7	20
80. $CH_3CO + Ar \rightarrow CH_3 + CO + Ar$	1.13×10^{15}	0	12.3	7.99×10^{12}	4.42×10^{13}	30.9	14.3	20
81. $C_2H_5 \rightarrow C_2H_4 + H$	3.62×10^{12}	0	37.2	1.14×10^{6}	2.07×10^{12}	24.9	38.3	12
82. $C_4H_3 \rightarrow C_4H_2 + H$	1.00×10^{14}	0	40.0	1.02×10^{7}	3.03×10^{13}	24.2	38.6	23
83. $C_4H_4 \rightarrow C_4H_3 + H$	2.00×10^{14}	0	103.0	1.97×10^{-4}	7.55×10^{12}	33.0	107.4	estd
84. $C_4H_3 + CH_3 \rightarrow C_4H_2 + CH_4$	3.92×10^{11}	0	0	3.92×10^{11}	4.94×10	−10.0	−69.2	estd
85. $C_4H_4 + CH_3 \rightarrow CH_4 + C_4H_3$	1.00×10^{13}	0	15.0	2.39×10^{10}	3.88×10^{10}	−1.24	−0.34	estd
86. $C_4H_3 + H \rightarrow C_4H_2 + H_2$	8.10×10^{13}	0	0	8.10×10^{13}	5.33×10^{2}	−3.45	−68.3	estd
87. $C_4H_4 + H \rightarrow C_4H_3 + H_2$	3.00×10^{14}	0	12.0	2.39×10^{12}	2.03×10^{11}	5.34	0.549	estd
88. $C_4H_4 + C_3H_3 \rightarrow p\text{-}C_3H_4 + C_4H_3$	1.00×10^{13}	0	15.0	2.39×10^{10}	7.62×10^{12}	0.014	14.3	estd
89. $C_4H_3 + C_2H_3 \rightarrow C_6H_5 + H$	5.00×10^{13}	0	15.0	1.19×10^{11}	6.25×10^{12}	−11.0	−3.94	estd
90. $C_4H_3 + C_2H_3 \rightarrow C_4H_4 + C_2H_2$	5.00×10^{11}	0	0	5.00×10^{11}	2.89×10	−9.17	−70	estd
91. $C_4H_3 + C_2H_3 \rightarrow C_4H_2 + C_2H_4$	5.00×10^{11}	0	0	5.00×10^{11}	8.41	−11.1	−75.5	estd
92. $C_6H_5 \rightarrow C_4H_3 + C_2H_2$	5.00×10^{14}	0	38.0	1.14×10^{8}	4.81×10^{12}	34.8	41.4	12
93. $C_3H_3 + C_3H_3 \rightarrow C_6H_6$	1.50×10^{13}	0	0	1.50×10^{13}	4.34×10^{-5}	−60.1	−146.8	estd
94. $C_3H_6 + H \rightarrow CH_3 + C_2H_4$	3.50×10^{14}	0	9.00	9.35×10^{12}	6.28×10^{9}	5.12	−11.7	estd
95. $C_2H_4 + H \rightarrow C_2H_3 + H_2$	1.33×10^{6}	2.53	12.2	6.59×10^{11}	2.58×10^{11}	7.67	7.25	13
96. $C_2H_4 + CH_3 \rightarrow C_2H_3 + CH_4$	6.63	3.70	9.50	4.16×10^{10}	3.12×10^{11}	1.09	6.37	13
97. $C_2H_4 + CH_3 \rightarrow nC_3H_7$	3.31×10^{11}	0	7.70	1.49×10^{10}	5.77×10^{7}	−29.9	−22.5	13
98. $n\text{-}C_3H_7 \rightarrow C_3H_6 + H$	1.80×10^{14}	0	38.2	3.77×10^{7}	1.45×10^{13}	24.8	34.2	12
99. $C_2H_6 + H \rightarrow C_2H_5 + H_2$	1.24×10^{14}	0	9.60	2.60×10^{12}	7.06×10^{9}	8.05	−4.62	12
100. $CH_3 + CH_3 \rightarrow C_2H_6$	1.01×10^{15}	−0.64	0	1.05×10^{13}	9.80	−40.3	−90.5	13

[a] $\Delta H_r°$ are expressed in units of kcal/mol and $\Delta S_r°$ in units of cal/(K mol), respectively. Rate constants are expressed as $k = AT^n \exp(-E/RT)$ in units of cm^3, s, mol, and cal. 2-mf is 2-methylfuran. 2-mfuryl is $(C_4H_3O)-CH_2^{\bullet}$.

SCHEME 5

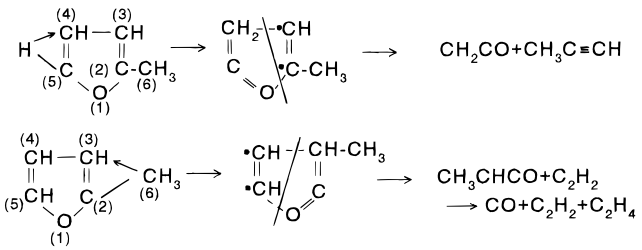

There are two additional unimolecular decomposition channels of 2-methylfuran. They involve the cleavage of other C—C bonds in the ring following the aforementioned 1,2 H-atom and 1,2 methyl group migrations (Scheme 5). These channels exist also in furan but owing to the symmetry of the molecule they appear as one channel.

The two channels in 2-methylfuran yield C_3H_4 (propyne and allene) with ketene in one channel and acetylene with CO and C_2H_4 in the second channel. Were the two channels completely equivalent, the second channel should have produced acetylene with methylketene, but as has been mentioned before we did not identify methylketene in the postshock mixtures and we thus believe that the latter immediately decomposes to ethylene and carbon monoxide.

$$CH_3(CH)C{=}O \rightarrow CO + C_2H_4$$

$$\Delta H_r°(298\text{K}) = 11.1 \text{ kcal/mol}$$

This observation is in complete agreement with the results of the computer simulation as the concentrations of C_2H_4 and C_2H_2 could not be accounted for without this channel. This will be discussed later.

b. Initiation of Free Radical Reactions. Free radical reactions are involved in the production of a large number of products such as CH_4, C_2H_6, and others. The C—H bond in the methyl group is the weakest bond in the molecule. It

is an sp^3 bond which is somewhat weakened by the $\beta-\gamma$ double bond bond of the ring, $D_{CH_2-H} \sim 90$ kcal/mol. The ejection of H-atom from the methyl group is thus the major initiator of free radical reactions. In addition to this process, as has been assumed in the past in similar 5-membered rings,[10,11] cleavage of the ring without H-atom or methyl group migrations can also take place. The three initiation reactions are reactions 7−9 in the reaction scheme, which is shown in Table 3.

In Figure 6 we compared the rates for total decomposition of 2-methylfuran and furan,[1] where the rate in 2-methylfuran is somewhat higher. We believe that this is the result of faster initiation of free radical reactions and faster H-atom abstractions owing to the existence of an sp^3 C—H bond in the methyl group. An equivalent C—H bond in furan does not exist.

c. Reaction Scheme and Computer Modeling. In order to account for the observed product distribution, we have constructed a reaction scheme containing 36 species and 100 elementary reactions. The scheme is shown in Table 3. The rate constants listed in the table are given as $k = AT^n \exp(-E/RT)$ in units of cm^3, mol, s, and cal. The Arrhenius parameters for the reactions in the scheme are based on experimentally deduced parameters and are estimated or taken from various literature sources, mostly from the NIST Kinetic Data Base.[12] The parameters for each reaction taken from the NIST Kinetic Data Base are the best fit to a large number of entries. (In view of the very large number of citations involved they are not given as references in the article.) Parameters for reactions which could not be found in available compilations are estimated by comparison with similar reactions for which the rate parameters are known.

The thermodynamic properties of the species involved were taken from various literature sources[13−16] or estimated with (SP).[9] We have performed sensitivity analysis with respect to variations (or rather uncertainties) in the ΔH_f° of species whose thermodynamic properties were estimated or are not known accurately enough. Incorrect values of the thermodynamic functions result in erroneous values for the rate constants of the back-reactions. In several sensitivity tests that were performed on the thermodynamic functions, we found that the results of the simulation were very insensitive to the estimated values.

The reactions that appear in the scheme, in addition to the unimolecular decompositions of 2-methylfuran, enter into several categories, among them radical−radical recombinations, abstraction and displacement reactions, unimolecular decomposition of unstable intermediates isomerizations, and others.

In the stage of constructing the scheme, we calculated the free radical profiles in order to determine which ones should be introduced into the scheme in abstraction and other reactions. The radical profiles of the final reaction scheme are shown in Figure 9. $CH_3^\bullet$ and $C_3H_3^\bullet$ have the highest concentrations among the free radicals in the system. In the H-atom abstraction reactions that appear in the scheme, particularly from the different C_4H_6 isomers and several other high-concentration products, we have considered only reactions of $CH_3^\bullet$, $C_3H_3^\bullet$, and $H^\bullet$.

The reaction scheme contains four unimolecular steps that produce carbon monoxide and four C_4H_6 isomers (1−4), two unimolecular steps that produce other stable molecules (5 and 6), and three unimolecular dissociations that produce unstable species (7−9). The latter initiate free radical reactions in the system. The scheme contains also four (out of six) interisomerizations of the various C_4H_6 isomers.[17] The reactions

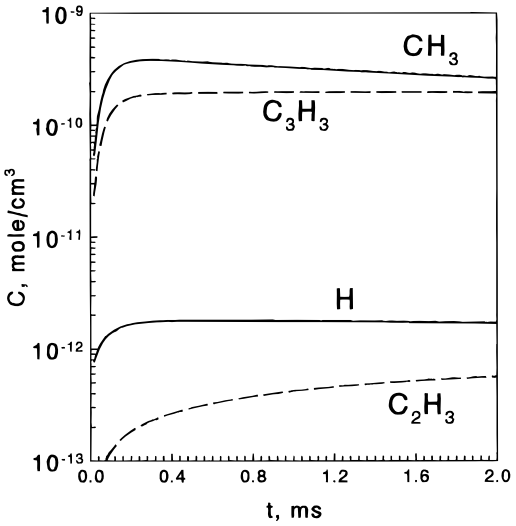

Figure 9. Calculated profiles of $CH_3^\bullet$, $C_3H_3^\bullet$, $H^\bullet$, and $C_2H_3^\bullet$ at 1250 K.

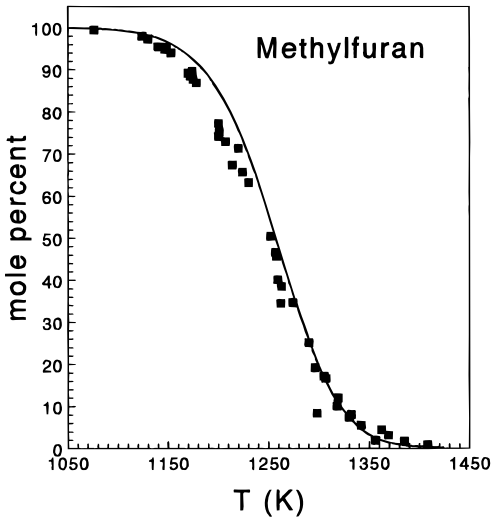

Figure 10. Experimental and calculated mole percents of the reactant 2-methylfuran.

$$CH{\equiv}CCH_2CH_3 \rightarrow CH_2{=}CHCH{=}CH_2$$

$$CH{\equiv}CCH_2CH_3 \rightarrow CH_3C{\equiv}CCH_3$$

cannot take place by simple rearrangements and do not appear in the scheme.

As has been mentioned before, the rate parameters for all of the reactions were either taken from various sources or were estimated. In the process of estimating rate parameters, we followed very strict rules such as, for example, *A* factors for recombinations and abstractions decrease as the size of the radicals increase, starting at $\sim 10^{14}$ cm^3 mol^{-1} s^{-1} for H-atoms and decreasing to $\sim 10^{10}-10^{11}$ cm^3 mol^{-1} s^{-1} for large radical species. Free radical dissociation is associated with stiff transition states and hence low *A* factors, *etc*.

Figure 10 shows the experimental and the calculated mole percent of 2-methylfuran corresponding to its overall decomposition. Figures 11−15 show experimental and calculated mole percents of products found in the decomposition of 2-methylfuran. The overall agreement seems to be quite satisfactory.

Table 4 (a and b) shows the sensitivity spectrum of the reaction scheme at 1150 and at 1300 K, respectively. The sensitivity factor $S_{i,j}$ is defined in the table as $\Delta(\log C_i)/\Delta(\log$

TABLE 4: Sensitivity Analysis (*k* Changed by a Factor of 3)

Reaction	CO	CH_4	C_2H_4	C_2H_6	C_2H_2	C_3H_6	*a*-C_3H_4	*p*-C_3H_4	CH_2CO	1,3-butadiene	2-butyne	1,2-butadiene	2-butyne	C_4H_4	C_4H_2	furan	C_6H_6
(a) At 1150 K																	
1											0.98						
2	0.42									0.98							
3												0.84					
4	0.35												0.97				
5								0.83	0.69								
6	0.22		0.98		0.97	0.71											
7		0.20		0.40		0.27	0.36							0.18	0.41		
9		0.42		0.81		0.61	0.31		0.27					0.55	0.99	0.60	0.63
10				−0.35										0.19		−0.24	0.29
11		0.52		−0.81		−0.20	0.20							0.28	0.19	0.20	0.44
12							−0.26	0.20									−0.58
13							0.66										−0.60
14						0.39											
16				0.20													
20				0.27			−0.25							0.23	0.29	0.18	−0.54
22				−0.32		−0.23	0.42		0.34					−0.30	−0.25	−0.20	0.86
23				0.26										0.22	0.32	0.17	−0.34
24							0.35										
36													0.18				
74						0.20											
75						−0.24											
78						0.36											
85															0.70		
87															0.22		
88															0.40		
93							−0.20										0.51
94						0.20											
96						0.20											
100		−0.29		0.37		−0.32									−0.30		
(b) At 1300 K																	
1											0.41						
2				−0.45		−0.48	−0.27	−0.29	−0.25	0.63		−0.21	−0.29	0.59			
3											0.18	0.26					
4	−0.30											0.34	0.59			−0.21	0.29
5							0.44	0.42	0.59						−0.25		
6			0.73		0.22	0.55									−0.21		
7				0.21													0.22
9				0.24						−0.20	−0.23				0.38	0.27	
10				−0.24													
14						0.26											
16				0.18												0.20	
17							0.23	0.23								−0.91	
22									0.27								0.25
25											−0.29						
26												−0.31					
27											0.28						
28												0.21	−0.24				
37				0.17										−0.58			
38											−0.41						
44													−0.25				
45											−0.32						
46		0.19								−0.32							
51													−0.23				
71			0.22							−0.20							
72					0.39									−0.58	−0.39		
75						−0.21											
78						0.35											
85															0.36		
87															0.58		
88															0.33		
96						0.29											
100		−0.23		0.27		−0.24											

k_j) at $t = 2$ ms. The sensitivity factors $S_{i,j}$ were evaluated by changing k_j by a factor of 3. Reactions that show no effect on the production rate of all of the products both at high and at low temperatures were not included in the tables.

Table 4 shows that only a relatively small number of elementary steps affect the product distribution in the sense that variation of their rates by a factor of 3, for example, affects at least the production rate of one of the products. The majority of the elementary reactions that compose the scheme do not affect the distribution at all. They are left in the kinetic scheme for the sake of completeness and applicability beyond the temperature range of the present experiments.

Most of the sensitivity factors that appear in Table 3 are self-explanatory and appear in many systems of the same nature. The sensitivity factors for reactions 7 and 100, for example, show the competition on methyl radicals which expresses itself in the production rates of methane vs ethane. The sensitivity factors for C_2H_2 and C_2H_4, as can be seen in Table 4, are high for reaction 6, which indicates that it is the main source for their production. The reaction has, however, only a mild effect on the production of CO because the latter also formed directly from the ring by other faster channels.

d. Existence of 1,2-Methyl Group Migration. After performing the computer simulation, we can better understand

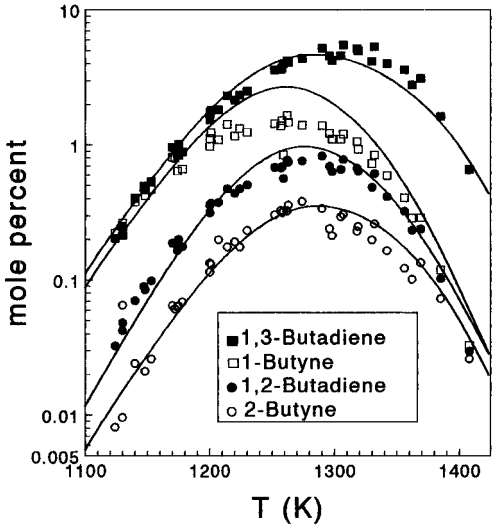

Figure 11. Experimental and calculated mole percents of the four C_4H_6 isomers.

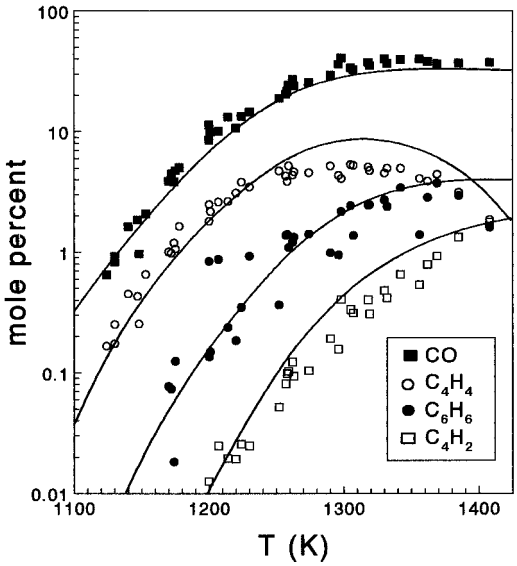

Figure 12. Experimental and calculated mole percents of CO, C_4H_4, C_6H_6, and C_4H_2.

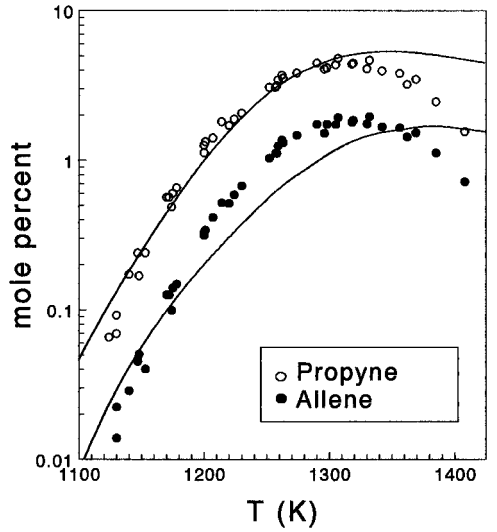

Figure 13. Experimental and calculated mole percents of propyne and allene.

and answer the question of whether the 1,2-methyl group migration from C(2) to C(3) in the ring is really necessary to explain the observed product distribution. This process accounts

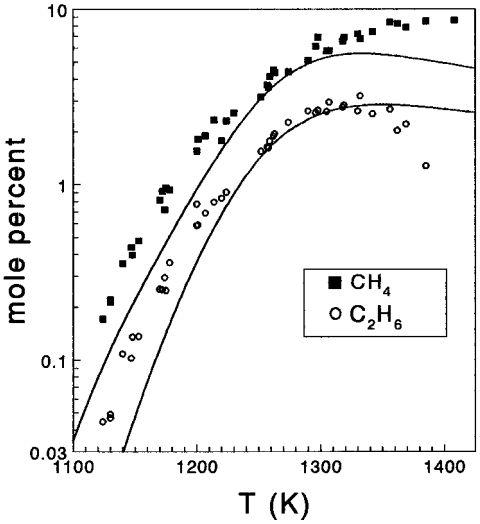

Figure 14. Experimental and calculated mole percents of methane and ethane.

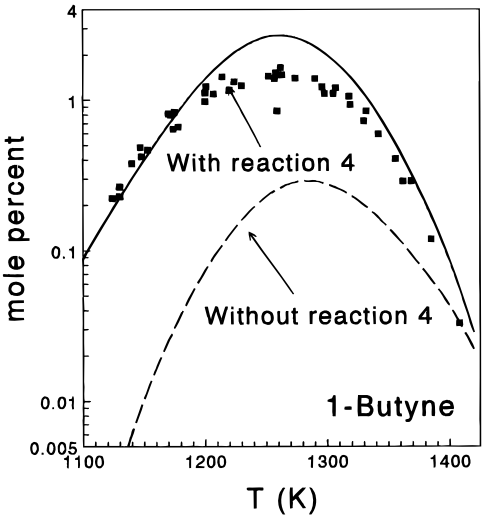

Figure 15. Experimental and calculated mole percents of 1-butyne with and without reaction 4. Isomerizations alone cannot account for the observed mole percent of 1-butyne.

for reactions 4 and 6. As has been shown, both can take place only after 1,2 methyl group migration from C(2) to C(3) in the ring has occurred. In reaction 4, 1-butyne is formed, and in reaction 6 acetylene and methylketene are formed, where the latter decomposes to carbon monoxide and ethylene.

1-Butyne. Since the four isomers of C_4H_6 can interisomerize,[17] it is possible, at least in principle, that 1-butyne is formed as a product of isomerization rather than directly from the 2-methylfuran ring. In order to clarify this point, we ran the kinetic scheme by eliminating reaction 4. The results are shown in Figure 15. It can readily be seen that, just by isomerization alone, 1-butyne cannot be obtained in large enough concentrations to match the experimental observation. This is particularly true at the lower temperature end. At high temperatures the concentrations of the isomers is high enough to produce the observed concentration of 1-butyne. These results are solid proof for the existence of the methyl migration channel.

C_2H_2 and C_2H_4. We ran the scheme without reaction 6. The results are shown in Figures 16 and 17. It can readily be seen that reaction 6 is necessary to produce enough C_2H_2 and C_2H_4. If this reaction is eliminated, the concentrations of C_2H_2 and C_2H_4 are too small as compared to the experimental values.

A byproduct of this observation is that methylketene decom-

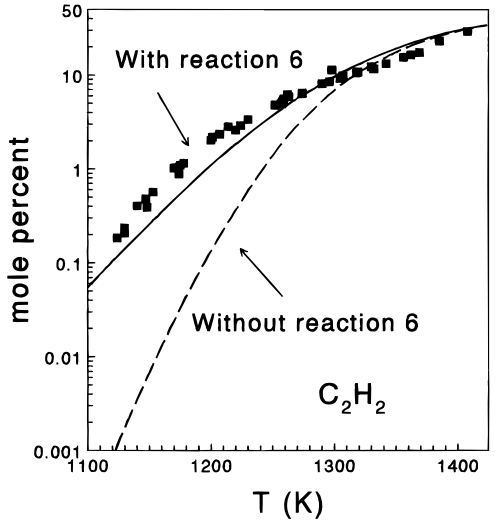

Figure 16. Experimental and calculated mole percents of C_2H_2 with and without reaction 6. Without this reaction which produces acetylene by a direct dissociation of the 2-methylfuran ring, its calculated mole percent is far below the experimental value.

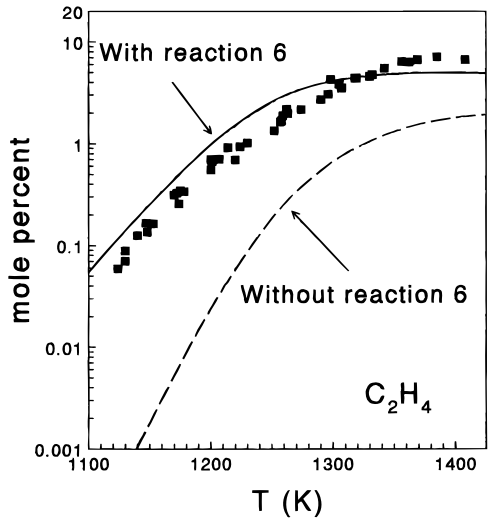

Figure 17. Experimental and calculated mole percents of C_2H_4 with and without reaction 6. Without this reaction, the relatively high mole percent of C_2H_4 cannot be accounted for.

poses completely and very fast to CO and C_2H_4 at the temperature range of this investigation.

1,2-Methyl group migrations have been shown to exist in other cyclopentadiene type rings, and the results obtained in this investigation are in complete agreement with them. 1,2-Methyl group migration from position 5 to position 4 in 5-methylisoxazole, which is isoelectronic to methylfuran, to produce CO and C_2H_5CN has recently been observed.[11] A similar migration has also been observed in 3,5-dimethylisoxazole.[18] On the other hand, Melius has recently expressed his inability to identify transition states involving 1,2 methyl group migrations in methyl cyclopentadienes.[24]

V. Conclusions

The decomposition pattern of 2-methylfuran is similar to that of furan. The loss of symmetry in the molecule opens more reaction channels which involve, in addition to hydrogen atom migration, a migration of the methyl group. The ring opening steps have high preexponential factors which point to the existence of biradical mechanisms. The computer modeling shows that the product distribution cannot be explained without assuming that a methyl group migration from position 2 to position 3 in the ring does takes place.

References and Notes

(1) Lifshitz, A.; Bidani, M.; Bidani, S. *J. Phys. Chem.* **1986**, *90*, 5373.
(2) Laskin, A.; Lifshitz, A. *Proceedings of the 20th International Symposium on Shock Tubes and Waves*; in press.
(3) Grela, M. A.; Amorebieta, V. T.; Collusi, A. J. *J. Phys. Chem.* **1985**, *89*, 38.
(4) Lifshitz, A.; Moran, A.; Bidani, S. *Int. J. Chem. Kinet.* **1987**, *19*, 61.
(5) Rogers, A. S.; Ford, W. G. F. *Int. J. Chem. Kinet.* **1973**, *5*, 965.
(6) *Eight Peak Index of Mass Spectra*; Mass Spectrometry Data Centre, The Royal Society of Chemistry, The University of Nottingham: Nottingham, U.K., 1983; ISBN 0-85186-407-4.
(7) Lifshitz, A.; Bidani, M.; Agranat, A.; Suslensky, A. *J. Phys. Chem.* **1987**, *91*, 6043.
(8) Lifshitz, A.; Frenklach, M.; Burcat, A. *J. Phys. Chem.* **1975**, *79*, 1148.
(9) Stein, S. E.; Rukkers, J. M.; Brown, R. L *NIST-Standard Reference Data Base 25*; National Institute of Standards and Technology: Washington, DC.
(10) Lifshitz, A.; Wohlfeiler, D. *J. Phys. Chem.* **1992**, *96*, 4505.
(11) Lifshitz, A.; Wohlfeiler, D. *J. Phys. Chem.* **1992**, *96*, 7367.
(12) Westly, F.; Herron, J. T.; Cvetanovic, R. J.; Hampson, R. F.; Mallard, W. G. *NIST-Chemical Kinetics Standard Reference Data Base 17, Ver. 5.0*; National Institute of Standards and Technology: Washington, DC.
(13) Tsang, W.; Hampson, R. F. *Phys. Chem. Ref. Data* **1986**, *15*, 1087.
(14) Melius, K. *BAC-MP4 Heats of Formation*; Sandia National Laboratories: Livermore, CA, March 1993.
(15) Pedley, J. B.; Taylor, R. D.; Kirby, S. P *Thermochemical Data of Organic Compounds*; Chapman and Hall: London, 1986.
(16) Burcat, A.; McBride, B.; Rabinowitz, M. *Ideal Gas Thermodynamic Data for Compounds Used in Combustion*; TAE 657 Report; Technion-Israel Institute of Technology: Haifa, Israel, 1994.
(17) Hidaka, Y.; Higashihara, T.; Ninomiya, N.; Oshita, H.; Kawano, H. *J. Phys. Chem.* **1993**, *97*, 10977.
(18) Lifshitz, A.; Wohlfeiler, D. *J. Phys. Chem.* **1995**, *99*, 11436.
(19) Hidaka, Y.; Nakamura, T.; Miyauchi, A.; Shiraishi, T.; Kawano, H. *Int. J. Chem. Kinet.* **1989**, *21*, 643.
(20) Warnatz, J. In *Rate Coefficients in the C/H/O System Combustion Chemistry*; Gardiner, W. C., Jr., Ed.; Springer-Verlag: New York, 1984; p 197.
(21) Benson, S. W. *Int. J. Chem. Kinet.* **1989**, *21*, 233.
(22) Fahr, A.; Laufer, A.; Klein, R.; Braun, W. *J. Phys. Chem.* **1991**, *95*, 3218.
(23) Weissman, M.; Benson, S. W. *Int. J. Chem. Kinet.* **1984**, *16*, 307.
(24) Melius, C. F. *26th Symposium (International) on Combustion*, Naples; The Combustion Institute: Pittsburgh, PA, 1996; paper 236.